A spin-filter made of quantum anomalous Hall insulator nanowires

Jiansheng Wu

Articles you may be interested in

A spin filter transistor made of topological Weyl semimetal
Appl. Phys. Lett. **107**, 102403 (2015); 10.1063/1.4930875

Quantum anomalous Hall effect and a nontrivial spin-texture in ultra-thin films of magnetic topological insulators
J. Appl. Phys. **117**, 17C741 (2015); 10.1063/1.4917006

Quantum anomalous Hall effect in topological insulator memory
J. Appl. Phys. **117**, 17C739 (2015); 10.1063/1.4916999

Electrically tunable spin filtering for electron tunneling between spin-resolved quantum Hall edge states and a quantum dot
Appl. Phys. Lett. **104**, 263101 (2014); 10.1063/1.4885040

Electrical switching of quantum tunneling through p-n junction in a quantum spin Hall bar
J. Appl. Phys. **113**, 053708 (2013); 10.1063/1.4790325

A spin-filter made of quantum anomalous Hall insulator nanowires

Jiansheng Wu
Department of Physics, South University of Science and Technology of China, Shenzhen,
People's Republic of China

Topological end states (TES) in quantum anomalous Hall insulator nanowires can induce tunneling within the gap. Such TES are spin polarized, thus the induced current is spin polarized as well, which can be used to construct a spin-filter applied in spintronics. An interferometry device is designed to control the polarized current as well. The advantage and finite size effect on this system are discussed. © 2014 AIP Publishing LLC. [http://dx.doi.org/10.1063/1.4891962]

Topological states, including topological insulator (TI) and topological superconductor (TSC), are new states of matter.[1,2] While in the bulk, TI (TSC) systems are gapped insulators (superconductors), they are metallic on the boundaries. These boundary states are protected by the non-trivial topology, which are so-called the topological boundary states (TBS). TBS bear some exotic properties which are not presented in normal insulator and normal superconductors. First, there exists non-trivial spin (or pseudospin) texture in TBS.[3–5] For example, topological end states (TES) of 1D class AIII TI, such as quantum anomalous Hall insulator (QAHI) nanowires, are polarized.[3] On the 1D boundary of 2D QAHI, there exists chiral spin texture.[5] Second, TBS also change the transportation properties of the system. For example, in the boundary or in the vortex center of TSC, there exist Majorana fermions, a kind of fermion of which the anti-particle is itself.[6–9] The presence of Majorana fermion will induce resonant Andreev reflection, in forms of zero-biased peak in the conductance,[10] in the normal metal-TSC-normal metal (NM-TSC-NM) heterostructure.

In this article, we make use of special properties of QAHI nanowires to construct a spin-filter (SF). The special properties come from the combination effect of both spin polarization[3] and the TES induced tunneling of QAHI nanowires. The later effect is similar to the Majorana fermion induced tunneling in TSC.[10] The TES of TI will also induce tunneling, modifying the transport properties of TI. Since TES are polarized, thus the TES induced tunneling current are polarized as well. So we applied such properties to make a spin-filter, a very important device in spintronics.

The Majorana fermions exist on the two boundaries of the TSC in the NM-TSC-NM heterostructure; they induce resonant Andreev reflection which can be measured by a zero-biased peak on the conductance. Similarly, to investigate the transport properties of the TI, we also consider a NM-TI-NM heterostructure. For simplicity, we consider a QAHI nanowire,[11,12] which belongs to 1D class AIII TI and can be simulated in cold atom system.[3] The Hamiltonian of such TI reads as[3]

$$\mathbf{H} = \sum_{\mathbf{k}} H(\mathbf{k}) = \sum_{\mathbf{k}} (\Gamma_z - 2t_s \cos k)\sigma_z + 2t_{so} \sin k \sigma_y. \quad (1)$$

Here, the basis is defined as $[c_\uparrow^\dagger, c_\downarrow^\dagger]|0\rangle$ where $|0\rangle$ is the vacuum, $c_{\uparrow,\downarrow}^\pm$ are creation and annihilation operator of electrons with spin *up* and spin *down* state. Γ_z is the

Zeeman energy, t_s is the spin-dependent hopping term, and t_{so} is the spin-orbital coupling. The energy spectrum of above Hamiltonian is given by $E_\pm(k) = \pm\sqrt{(\Gamma_z - 2t_s \cos k)^2 + (2t_{so} \sin k)^2}$. This system satisfies the chiral symmetry (CS) $\mathbb{C} = \sigma_x$ which is subject to the relation $\mathbb{C}H(\mathbf{k})\mathbb{C}^{-1} = -H(\mathbf{k})$. So it belong to the class AIII (chiral unitary) TI with topological number $\mathbb{Z}$. In this system, there exists one TES on each end when $\Gamma_z < 2t_s$ (topological number $N = 1$ by calculating the winding number[3]) while no TES exist otherwise ($N = 0$). If the length scale L of the middle region is the dominant length scale, by solving the eigenequation, the wavefunction of zero energy TES on the left end is in forms of $f_-(x) = \frac{1}{\sqrt{2}}[1, -1]u(x)$ and zero energy TES on right end is $f_+(x) = \frac{1}{\sqrt{2}}[1, 1] u(L - x)$. So they are eigenstates of spin operator S_x. The spatial part of the wavefunction is $u(x) \propto (e^{-\lambda_+ x} - e^{-\lambda_- x})$ with $\lambda_\pm$ such that $t_s\lambda^2 - t_{so}\lambda - (\Gamma_z - 2t_s) = 0$. We can see if $\Gamma_z - 2t_s < 0$, two solutions $\lambda_\pm$ are with positive real part. Thus, wavefunction of zero energy state satisfying fixed boundary conditions exists. The above criteria agree with the previous calculation from winding number. TES localize on two ends with the localization length $\xi = 2t_s/t_{so}$. If ξ is comparable with L, two TES overlap with each other and this induce coupling between them, leading to the TES induced tunneling.

The presence of the TES changes the transportation properties of the TI region. We use lattice Green function to calculate the conductance of TI in the NM-TI-NM heterostructure.[13] When a fermion from left lead in the eigenstate of S_b ($b = \{x, y, z\}$) with eigenvalue ν ($\nu = \pm$), denoted as polarization νb, is transmitted through TI to state with polarization μa on the right lead, the transmission coefficient (TC) $T_{\sigma a, \nu b}$ can be obtained by[13,14]

$$T_{\sigma a, \nu b}(E) = \text{Tr}(\mathbf{\Gamma}_{R\sigma} \mathbf{G}_{\sigma,\nu}^r \mathbf{\Gamma}_{L\nu} \mathbf{G}_{\sigma,\nu}^a). \quad (2)$$

Here, the vertex operator is $\mathbf{\Gamma}_{c\sigma}(E) = i[\mathbf{\Sigma}_{c\sigma}^r(E) - \mathbf{\Sigma}_{c\sigma}^a(E)]$ ($c = \{L, R\}$ is the index of the left/right lead) and the retarded (advanced) Green functions are defined as $\mathbf{G}^r(E) = [\mathbf{G}^a]^\dagger = 1/[E - \mathbf{H} - \sum_c \mathbf{\Sigma}_c^r]$. The retarded self-energy $\mathbf{\Sigma}_c^r(E)$ is due to the coupling to the leads which can be calculated by iteration numerically.[13,14] From the calculated TC, the particle current in the left lead with certain polarization can be obtained by the Landauer-Buttiker formula.[13] We

consider the zero temperature case and assume that the chemical potential of both sides is the same and spin independent. The hopping energy from NM to TI is set to $t = 0.2t_s$ and $t_{so} = 10t_s$, and TC for incident electrons with polarization $\pm x$ is calculated, respectively. TC at zero temperature is obtained in Fig. 1.

We found that within the gap, TC $T_{+x,-x}$ as well as conductance have one peak or two peaks for given Γ_z. The distance of two peaks (energy split) at given Γ_z is an oscillating function of Γ_z. This energy split is roughly the energy scale of the coupling energy of two TES. Since the TES are oscillating function in space and the oscillating wave vector is determined by the energy gap depending on Γ_z. Their coupling energy due to the overlap of wavefunction oscillates as well leading to an oscillating energy split. Such energy split appears in the Majorana fermion induced tunneling as well.[15] Second, we can see the nonzero conductance within the gap disappears at $\Gamma_z = \pm 2t_{so}$ which is due to the close of the gap. Furthermore, we found that for given Γ_z and E, $T_{+x,-x}$ is much higher than the other TCs. This agrees with the fact that the TES on both ends are polarized in $+x$ and $-x$, respectively. Within four possible combinations of incident polarization and outgoing polarization, we found that within the gap, at the same E and Γ_z values, $T_{+x,-x} \gg T_{-x,-x} \approx T_{+x,+x} \gg T_{-x,+x}$. This is different from the long wire case, which we should have $T_{+x,-x} = 1$ and zero for other TC. It is due to finite size effect: the left (right) TES have a nonzero tail on the right (left) end, so the polarizations of TES are no longer along $\pm x$, i.e., they have been tilted from $\pm x$ by a small angle which lead to nonzero $T_{-x,-x}$, $T_{+x,+x}$ and $T_{-x,+x}$. This can be more apparent by using an effective model in the following.

We can also calculate the above conductance by using the effective Hamiltonian and the scattering matrix.[14] The effective Hamiltonian for this spin-polarized zero mode assisted tunneling can be read as

$$H = H_L + H_{TI} + H_T + H_t$$
$$= -iv_F \int dx \psi^\dagger_{\pm L}(x) \partial_x \psi_{\pm L}(x) - iv_F \int dx \psi^\dagger_{\pm R}(x) \partial_x \psi_{\pm R}(x)$$
$$+ E_0 f^\dagger_+ f_- + w_1 f^\dagger_{-L} \psi_{-L}(0) + w_2 f_{+R} \psi^\dagger_{+R}(L)$$
$$+ t_1 f^\dagger_{+R} \psi_{+L}(0) + t_2 f_{-L} \psi^\dagger_{-R}(L) + hc, \quad (3)$$

where $c^\pm_{L,R}$ are the electron creation and annihilation operators on the left and right leads, respectively, $f^\pm_\pm$ are the creation and annihilation operator of spin-polarized zero mode, $w_{1,2}$ are hopping energy without spin flipping, and $t_{1,2}$ are hopping energy with spin flipping. Due to finite size effect, a TES localized on left (right) end has a nonzero tail on the right (left) end, so $t_{1,2}$ are nonzero but is much smaller than $w_{1,2}$. The scattering matrix element (SME) of the transmission and reflection is calculated by the method of Beenakker et al.,[10,16] the conductance at zero temperature is obtained as

$$G \approx \frac{e^2}{h} \frac{1}{[E^2 - (E_0^2 - \Gamma^2)]^2 + 4E_0^2\Gamma^2}$$
$$\times \begin{bmatrix} 4E_0\Gamma\delta\sqrt{E^2 + (\Gamma+\delta)^2} & 4\Gamma^2 E_0^2 \\ 4\delta^2 E_0^2 & 4E_0\Gamma\delta\sqrt{E^2 + (\Gamma+\delta)^2} \end{bmatrix},$$
$$(4)$$

where $\Gamma_i = |w_i|^2/v_F$, $\delta_i = |t_i|^2/v_F$ (v_F is the Fermi velocity of NM) and we assume $\Gamma_1 = \Gamma_2 = \Gamma$, $\delta_1 = \delta_2 = \delta$, and $\delta \ll \Gamma$.

The leading order of TC is got by setting $\delta = 0$. $\delta = 0$ is for the case of the long wire ($L \gg \xi$), where the tail of left (right) TES on right (left) end can be ignored. At zero temperature, the tunneling conductance can be obtained as follows, if assuming that on both leads, chemical potential is all equal to zero for all spin polarization, $\sigma_{+x,-x} = \frac{e^2}{h} 4E_0^2\Gamma^2 / [(E^2 - \epsilon_0^2)^2 + 4E_0^2\Gamma^2]$. The only nonzero conductance is $T_{+x,-x}$. It is a TES induced tunneling effect. We can see for strong coupling case ($E_0 > \Gamma$), TC has double peaks at $\pm\epsilon_0 = \pm\sqrt{E_0^2 - \Gamma^2}$ with peak values one (for the extremely strong coupling case, δ should be taken into account; the above formula is not accurate), while for weak coupling case ($E_0 \leq \Gamma$), TC within gap only peaks at $E = 0$ with peak values less than one. Γ is fixed for given hopping energy w from leads to sample; E_0 is affected by the system size L. As L increase, E_0 decrease, we can see the transition from double peaks to single peak, which is illustrated in Fig. (2). Furthermore, the half width of the peak $2E_0\Gamma$
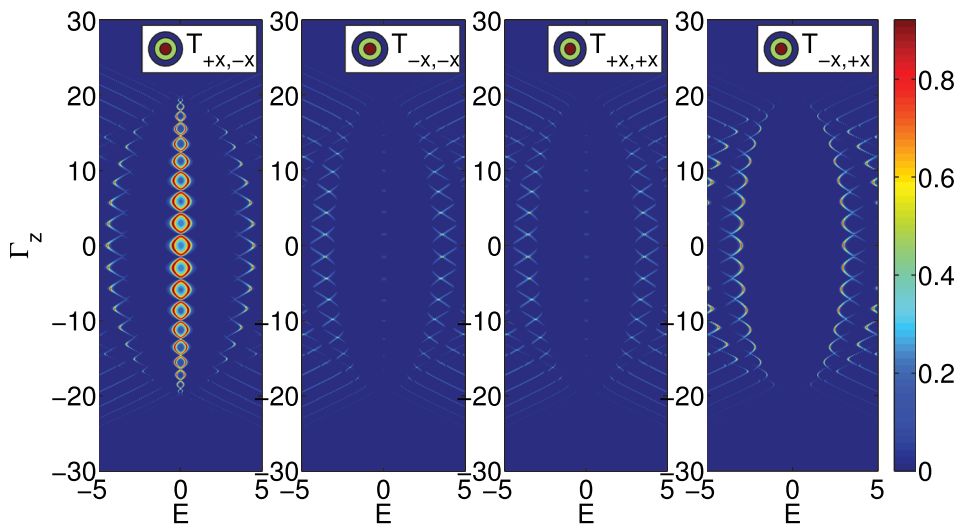

FIG. 1. Transmission coefficient as a function of Γ_z and E for fermions with different incoming and outgoing polarizations. From left to right, figures are for $T_{+x,-x}$, $T_{-x,-x}$, $T_{+x,+x}$, and $T_{-x,+x}$.
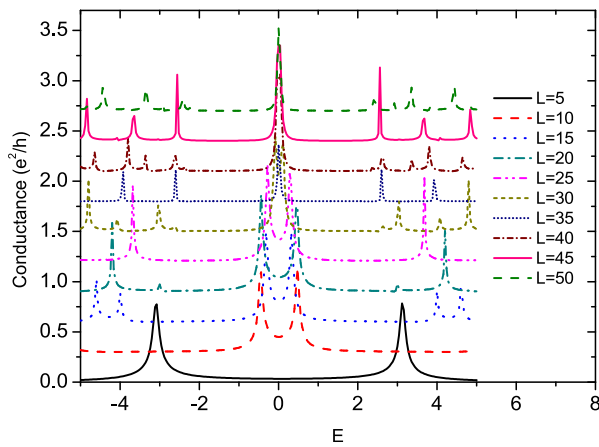
FIG. 2. Conductance vs energy E for varies of system size L (zero point of conductance is shifted upward by 0.3 on the top of the previous values for clarification). The parameters are set as $\Gamma_z = 3.4t_s$, $t_{so} = 10t_s$, and $t = 0.1t_s$.
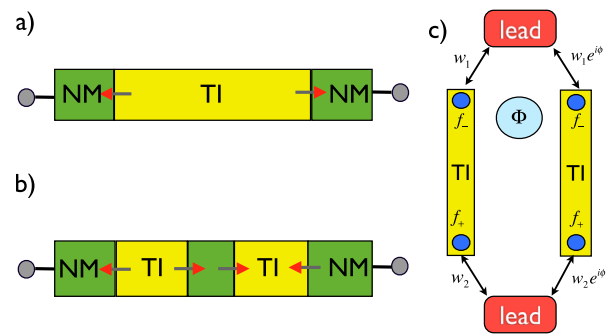

FIG. 3. Spin-filter and an interferometry device to control polarized current. (a) two-terminal SF. Left (right) red arrow represents the $-x/+x$ polarized TES. (b) A polarization $-x$ to polarization $-x$ SF, which is made of two spin flip filter with opposite Chern number. (c) A interferometry device made of two class AIII TI, top and bottom rectangular are two leads. The left and right yellow wires are two TI nanowires with two TES, respectively. Φ is the inserted magnetic flux.

decreases with larger system size. The fermions with $+x$ polarization cannot tunnel through the TI, i.e., $R_{+x} = \infty$. Thus, the magnetoresistance ratio (MRR) or relative resistance change is as MRR $= (R_{-x} - R_{+x})/R_{-x} \to \infty$. As mentioned above, the TES are completely polarized along x direction in the long wire limit (weak coupling). If the length is not sufficient long, the polarization is tilted to a small angle (denoted as θ) from x-direction. So $T_{\pm x, \pm x}$ and $T_{-x,+x}$ are nonzero as well. The new polarization direction of TES can be obtained by diagonalizing the conductance matrix. Thus, at $E = 0$, the tilted angle can be obtained as $\tan\theta \approx \delta/E_0$. If we still use the $\pm x$ as the incident and outgoing polarization, TC can be approximated as $T_{+x,-x} = T_0^2 \cos^4\theta$, $T_{\pm x, \pm x} = T_0^2 \sin^2\theta \cos^2\theta$, and $T_{-x,+x} = T_0^2 \sin^4\theta$ with $T_0 \equiv t_{+\theta,-\theta}$. For $\theta \ll \pi$, we can see that these results agree with the numerical simulations. And the MRR is MRR $\approx \cot^2\theta - 1 \approx E_0^4/\delta^4$.

From above, we can see even for an unpolarized incident current, the outgoing currents through NM-TI-NM heterostructure are polarized. So we can use the above combined effect of TES induced tunneling and nontrival polarization of TES to make SF: Such device opens a channel only for $-x$ polarization to $+x$ polarization. Furthermore, we can add two such structures with opposite Chern number to make $+x$ polarization to $+x$ polarization and $-x$ polarization to $-x$ polarization SF (as illustrated in Fig. 3).

The ordinary spin-filter is made of giant magnetoresistance (GMR) which make use of spin-dependent scattering if the middle layer is metal (so-called spin valve device, SVD) or spin-dependent tunneling if the middle layer is insulator (so-called magnetic tunneling junction, MTJ).[17] However, our SF is based on totally different mechanism in which TI

is used as a filter. It has several advantages. First of all, it has a high MRR and still low resistance, while SVD and MTJ can have one of these two properties. Second, SF here does not need to establish the parallel and anti-parallel magnetization of magnetoresistance devices, which require complicate fabrications and operations. Furthermore, in the real systems of conventional SF, the middle normal metal layer or insulating layer has much small conductivity compared with the magnetized layers which lead to undistinguishable up-spin and down-spin conductivity as well as the undistinguishable up-spin current and down-spin currents. So the polarization of current fails which is the so-called conductivity mismatch problem.[17] However, such problem would not appear in SF using TI. Third, the MRR is tunable if we tune localization length of SF by tuning Γ_z. This is important since a suitable MRR is needed for good current drivability for the close channel. Last but not the least, the spin-flip problem in the middle layer of GMR is no longer a problem here, since TES are not affected by the spin-flip process within TI. The above advantages make the SF using TI a promising candidate for future spintronics device using topological materials.

To control the spin polarized current, we consider two nanowires of class AIII TI connected in the way illustrated in Fig. 3(c). Both nanowires support one TES on each end. We consider the case that both nanowires have the same positive Γ_z, t_s, and t_{so}. In this case, four TES are in the state shown in the figure (for simplicity, we assume $\delta = 0$ in both nanowires). Arbitral incoming fermion can be decomposed into a combination of $+x$ and $-x$ states. The first component is totally reflected on both nanowires and the second one is transmitted by the left or right wire into $+x$ on the corresponding ends. Then, these states by two channels are recombined again, and the conductance is

$$\sigma_{+x,-x} = \frac{e^2}{h} \frac{4(\cos^2\phi)(E^2 - E_0^2)^2 E_0^2 \Gamma_1 \Gamma_2}{\left[-E_0^2 \Gamma_1 \Gamma_2 \sin^2\phi + (E^2 - E_0^2)(E^2 - E_0^2 - \Gamma_1 \Gamma_2)\right]^2 + (E^2 - E_0^2)^2 E^2 (\Gamma_1 + \Gamma_2)^2}, \quad (5)$$

where $\phi = \Phi/2\Phi_0$ and Φ_0 is flux quantum and Φ is magnetic flux. We can control the outgoing polarized current by tuning the inserted magnetic flux.

The QAHI nanowires have two polarized TES which can induce tunneling within the energy gap. We use such systems to construct a spin-filter which can filter the unpolarized spin current to generate a polarized one with a very high magnetoresistive ratio. An interferometry device made of two nanowires is designed to control the polarized spin current. Such new device made of topological materials has many advantage compared with the ordinary spin-filter and is the new direction of spintronics device.

[1] M. Z. Hasan and C. L. Kane, Rev. Mod. Phys. **82**, 3045 (2010).
[2] X.-L. Qi and S.-C. Zhang, Rev. Mod. Phys. **83**, 1057 (2011).
[3] X.-J. Liu, Z.-X. Liu, and M. Cheng, Phys. Rev. Lett. **110**, 076401 (2013).
[4] J. J. He, J. Wu, T.-P. Choy, X.-J. Liu, Y. Tanaka, and K. T. Law, Nat. Commun. **5**, 3232 (2014).
[5] J. Wu, J. Liu, and X.-J. Liu, e-print arXiv:1401.0415.
[6] E. Majorana, Nuovo Cimento **14**, 171 (1937).
[7] L. Fu and C. L. Kane, Phys. Rev. Lett. **100**, 096407 (2008).
[8] R. M. Lutchyn, J. D. Sau, and S. Das Sarma, Phys. Rev. Lett. **105**, 077001 (2010).
[9] J. Alicea, Rep. Prog. Phys. **75**, 076501 (2012).
[10] K. T. Law, P. A. Lee, and T. K. Ng, Phys. Rev. Lett. **103**, 237001 (2009).
[11] X.-L. Qi, T. L. Hughes, and S.-C. Zhang, Phys. Rev. B **82**, 184516 (2010).
[12] C.-Z. Chang, J. Zhang, X. Feng, J. Shen, Z. Zhang, M. Guo, K. Li, Y. Ou, P. Wei, L.-L. Wang et al., Science **340**, 167 (2013).
[13] S. Datta, Electronic Transport in Mesoscopic Systems (Cambridge University Press, Cambridge, England, 1995).
[14] D. H. Lee and J. D. Joannopoulos, Phys. Rev. B **23**, 4997 (1981); M. P. Lopez Sancho, J. M. Lopez Sancho, J. M. L. Sancho, and J. Rubio, J. Phys. F **14**, 1205 (1984); **15**, 851 (1985).
[15] S. Das Sarma, J. D. Sau, and T. D. Stanescu, Phys. Rev. B **86**, 220506 (2012).
[16] J. Nilsson, A. R. Akhmerov, and C. W. J. Beenakker, Phys. Rev. Lett. **101**, 120403 (2008).
[17] S. Sugahara and J. Nitta, Proc. IEEE **98**(12), 2124 (2010).